

Modeling-Assisted InSAR Phase-Unwrapping Method for Mapping Mine Subsidence

Yiwei Dai, Alex Hay-Man Ng^{ID}, Hua Wang^{ID}, Liyuan Li^{ID}, Linlin Ge, and Tingye Tao

Abstract—Compared with traditional measurement technologies, synthetic aperture radar interferometry (InSAR) has unique advantages in monitoring ground subsidence due to underground mining. However, when the subsidence gradient of the subsidence trough exceeds the maximum measurable gradient of InSAR technology, the interference fringes will be too dense, causing phase aliasing. As a result, it is impossible to obtain correct phase-unwrapping result. The main objectives of this letter are two folded. First is to develop an unwrapping strategy to deal with the unwrapping problem caused by large subsidence gradient at the mine subsidence trough. The main idea of this strategy is to estimate most of the subsidence phase by multiple model inversions based on iterative approach. Then, the model phases from multiple models are combined with the final unwrapped residual phase. Another objective of this letter is to evaluate the feasibility of the three common deformation models, i.e., Mogi, probability integral method (PIM), and Okada, in solving the phase-unwrapping problem. Their advantages and disadvantages are outlined. Both the simulated data and real data are used for this experiment. The result shows that the problem of large subsidence gradient in the differential interferometric synthetic aperture radar (DInSAR) results can be solved by multiple model inversion. Among the three models, the use of Okada model seems to provide slightly more accurate result for solving the large-scale subsidence in the mining area than the other two models with the proposed strategy.

Index Terms—Differential interferometric synthetic aperture radar (DInSAR), mine subsidence, phase-unwrapping, subsidence model.

I. INTRODUCTION

SYNTHETIC aperture radar interferometry (InSAR) technology makes use of microwave band characteristics for coherent imaging. It can observe terrain [1], [2] and monitor surface deformation caused by crustal movement [3]–[5] and underground resource exploitation [6]–[10]. The use of InSAR

Manuscript received November 3, 2019; revised December 17, 2019 and March 9, 2020; accepted April 28, 2020. Date of publication May 14, 2020; date of current version May 21, 2021. This work was supported in part by the Natural Science Foundation of Guangdong Province under Grant 2018A030310538 and in part by the Science and Technology Program of Guangzhou under Grant 201904010254. (*Corresponding author: Alex Hay-Man Ng.*)

Yiwei Dai, Alex Hay-Man Ng, Hua Wang, and Liyuan Li are with the Department of Surveying Engineering, Guangdong University of Technology, Guangzhou 510006, China (e-mail: ywdai1026@163.com; hayman.ng@gmail.com; ehwang@163.com; gdliyuan@hotmail.com).

Linlin Ge is with the School of Civil and Environmental Engineering, University of New South Wales, Sydney, NSW 2052, Australia (e-mail: l.ge@unsw.edu.au).

Tingye Tao is with the School of Civil Engineering, Hefei University of Technology, Hefei 230009, China (e-mail: cztyt@163.com).

This article has supplementary downloadable material available at <https://ieeexplore.ieee.org>, provided by the authors.

Color versions of one or more of the figures in this letter are available online at <https://ieeexplore.ieee.org>.

Digital Object Identifier 10.1109/LGRS.2020.2991687

technology to monitor the deformation caused by coal mining has important economic and social significance.

Underground mining usually results in large subsidence on the surface of ground, which has been one of the main issues that limit the capability of InSAR technology in mine subsidence monitoring application. InSAR has achieved many successful examples in mine subsidence monitoring applications [8]. However, when the magnitude of mine subsidence exceeds the maximum measurable gradient of InSAR technology, the interferometric fringes are too dense to meet the requirements of Nyquist sampling theorem, causing the interference phase aliasing phenomenon (the term phase saturation will be used in this letter) [11]. Therefore, the correct phase-unwrapping result cannot be obtained. In many cases, only the rim of the subsidence trough can be unwrapped, where the center of the subsidence trough will become disordered. Many researches by various scholars have been attempted to overcome this problem, which can be divided into the following three types.

- 1) Optimize the algorithm of InSAR itself, such as oversampling [12], interpolation [13], and the shortest time baseline interference combination [8]. Although the phase-unwrapping error rate can be reduced to a certain degree, these methods are limited by the satellites' configurations and cannot fundamentally solve the phase saturation issue.
- 2) Combine InSAR technology and other deformation monitoring technologies such as 3-D laser scanning technology [14] and SAR pixel offset tracking (POT) [15]. However, these methods require a lot of manpower, material resources, and financial resources, and sometimes the monitoring environment cannot be satisfied because of the harsh environment of the mining area. In addition, the accuracies of these technologies are often poorer than InSAR measurements.
- 3) Combining InSAR technology with mine subsidence model such as probability integration method [16], [17], logistic model [18], and Knothe–Budryk model [9]. Although these methods can estimate the signal of large gradient subsidence by a subsidence model, the deformation value obtained by these methods is the predicted value of the model rather than the real and effective observation value. To some extent, it can solve the problem, but it cannot guarantee that the model results can represent the real subsidence situation. Diao *et al.* [19] and Fan *et al.* [20] proposed to use the subsidence model to predict the mine subsidence using the known geological mining parameters

and subtracted them from the InSAR phase to obtain the residual phases. Since large-scale subsidence signal has been removed, the success rate for unwrapping the residual phases can be greatly improved. Actual subsidence values can, hence, be obtained by combining the modeled subsidence and the unwrapped InSAR residual phases. Since the accuracy of subsidence model can be largely affected by the uncertainties of the model parameters [21], this approach is greatly limited by the model imperfection and the reliability of geological parameters used. Therefore, phase saturation issues can still be observed in some of the residual phase results.

A general approach is, hence, necessary to solve the phase saturation problem. In this letter, we propose to separate large gradient and small subsidence signals by iteratively inverting deformation models. The real deformation can then be retrieved by adding the modeled and the residual signals. In this letter, we investigated three widely used models, i.e., Mogi [22], Okada [23], and probability integral method (PIM) [24]. Our method can well solve phase saturation problems without knowing the precise geological mining parameters, so that it can be operationally used in mining subsidence applications.

II. METHODOLOGY

A. InSAR Processing

In general, the interference phase in a single interferogram mainly consists of the deformation phase, the terrain phase, the orbital phase, atmospheric phase, and the decorrelation noise [4]. In this letter, the two-pass differential interferometric synthetic aperture radar (DInSAR) technique [3] was used to remove the terrain phase by using the 1 arcsec Shuttle Radar Topography Mission (SRTM) digital elevation model (DEM) [2]. Because the area affected by underground mining is relatively small [25], orbital errors and a small amount of atmospheric delay errors were simply removed as a linear trend using far-field observations. In order to minimize the noise, adaptive filtering [26] was applied. The unwrapping strategy for mine subsidence mapping developed in this letter was then conducted to obtain the unwrapped deformation phase.

B. Constructing the Functional Relationship Between Model and InSAR

InSAR and geometric model were fused to establish the relationship among them. For a side-view satellite SAR system, InSAR observes surface deformation along the line-of-sight (LOS). The LOS deformation D_{LOS} is actually composed of the vertical D_u , easting D_e , and northing D_n displacement components [27]–[29]

$$D_{\text{LOS}} = D_u \cos \theta + D_n \sin \alpha_h \sin \theta - D_e \cos \alpha_h \sin \theta \quad (1)$$

where θ is the incidence angle and α_h is the azimuth of the satellite's flight direction.

C. Establish the Fitness Function of the Genetic Algorithm

The vertical displacement D_u , the easting displacement D_e , and the northing displacement D_n calculated by the three

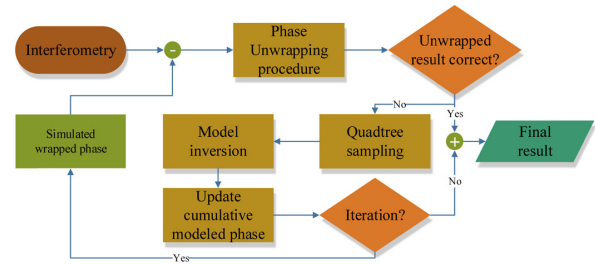


Fig. 1. Processing flowchart.

deformation models, Mogi, Okada, and PIM, can be used to derive the predicted LOS displacement based on (1).

Assuming that there are m observation points available, the residual LOS displacement can be obtained at any observation point i . Then the sum of the square of the residuals of m observation points is

$$S = \sum_{i=1}^m (D_{\text{InSAR}_i} - D_{\text{Model}_i})^2 \quad (2)$$

where D_{InSAR} is the InSAR-derived LOS displacement and D_{Model} is the LOS displacement derived from the subsidence model. In this letter, the minimization of S is obtained using genetic algorithm (GA) [30] to invert the parameters of the subsidence model.

D. InSAR Phase-Unwrapping Strategy for Mine Subsidence Mapping

Local large gradient deformation in a single interferogram can lead to problems such as loss of coherence, phase-unwrapping errors, and inaccurate coherence estimates. This letter focuses on solving the large gradient deformation problem in each interferogram, thus improving the success rate of phase-unwrapping and the accuracy of coherence estimation.

In this letter, an unwrapping strategy is developed to deal with the phase saturation problem for mine subsidence monitoring. The idea of the strategy is the mine subsidence trough, usually elliptical or circular in shape [31], can be represented as a sum of elliptical or circular deformation bowls. Therefore, multiple inversions of deformation models can be applied to minimize the impacts due to model imperfection and inaccurate geological parameters used. The specific steps are shown in Fig. 1 and explained below.

- 1) In this letter, SNAPHU (Statistical-cost, Network-flow Algorithm for Phase Unwrapping) [32] is used to unwrap the interferogram for model inversion. Other unwrapping methods can also be applied, but SNAPHU is chosen here because minimal manual involvement is needed. Ideally, the subsidence center should be masked to avoid errors in model inversion. However, based on our experiences, the results obtained with the subsidence center masked or not have little effect on the final results.
- 2) Because of the high density of observation points from unwrapped InSAR phase, spatial subsampling is preferred to reduce the computation resources required to invert large amount of data. The quadtree algorithm [33],

a popular down-sampling algorithm for InSAR modeling, is used in this letter. The down-sampled interferogram usually gives denser measurements in the near field where the deformation gradient is higher than the far field [33].

- 3) GA is then used to invert parameters of the subsidence model (see Appendix S1 for the descriptions of the three deformation models, i.e., Mogi, Okada, and PIM). This strategy attempts to gradually remove large-scale deformation signal based on iterative approach, therefore the starting point and upper/lower bounds of the parameters used for inversion do not need to be very precise.
- 4) The inversion parameters are used to simulate the subsidence trough.
- 5) The residual phase is obtained from the difference between the modeled phase and the interferogram from (1). Adaptive filter is applied to the residual phase for noise reduction.
- 6) Repeated (1)–(5) but with phase from (5) as input until the residual phase is completely unwrapped or the model cannot be further used to remove the residual phase.
- 7) The final deformation is determined by adding the modeled surface deformation from each iteration to the residual deformation.

III. SIMULATION EXPERIMENT

A. Data Simulation

A mine subsidence trough was simulated by Okada model based on the historical subsidence data from the Metropolitan mine, Australia. The model parameters used to simulate the mine subsidence trough are as follows: depth = 200.23 m, strike angle = 94.93°, dip angle = 7.95°, fault length = 136.98 m, fault width = 72.63 m, strike slip component = -0.58 m, dip slip component = -1.26 m, and tension slip component = 1.87 m. The simulated data were added with different levels of Gaussian noise of 3, 5, and 7 mm. The simulated mine subsidence trough was then normalized. The purpose of normalization processing is to detect the maximum subsidence that can be unwrapped by the proposed method. Normalization was applied to the simulated subsidence trough according to its peak subsidence values. Since mine subsidence is mostly elliptical or circular in shape, the shape of subsidence here was kept consistent in this simulation with varying subsidence gradient as variable. The subsidence troughs with a peak subsidence from 1 to 35 cm were simulated based on the approach used in [13] and [25]. The simulated subsidence troughs with different noise levels and peak subsidence were rewrapped into an interferogram with a C-band wavelength of 5.55 cm.

B. Experiment With the Interferogram Generated From the Okada Model

The phase-unwrapping strategy developed in this letter is applied to the simulated subsidence troughs. Three models, Mogi, PIM, and Okada, are inverted using GA.

Fig. 2 shows the case when the Gaussian error of 3 mm is added with the peak subsidence of 35 cm (79.2 rad). After two inversions of the Mogi model, the center phase of the

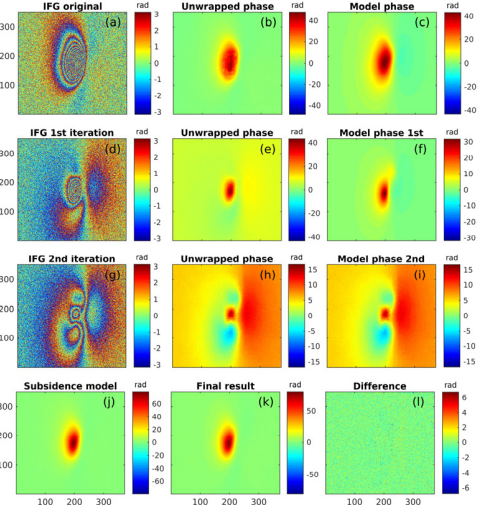


Fig. 2. Result from the Mogi model based on the simulation of a subsidence trough with 3-mm error and a peak subsidence of 35 cm. (a) Original interferogram and (d) and (g) residual interferogram after the first and second iterations, respectively. (b), (e), and (h) Unwrapped phase of (a), (d), and (g), respectively. (c) and (f) Modeled phase of (b) and (e), respectively. (i) Same as (h) for the convenience of comparison. (j) Simulated subsidence trough. (k) Final result obtained using the proposed strategy. (l) Difference between (j) and (k).

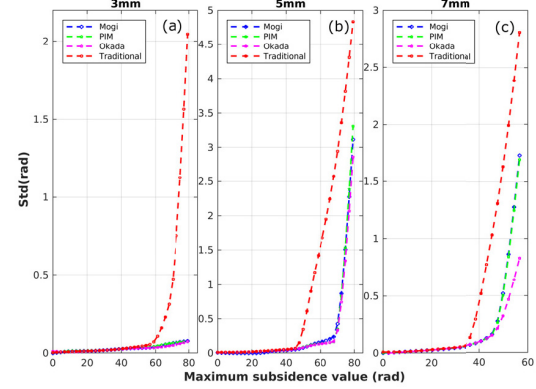


Fig. 3. Comparison of Mogi, PIM, and Okada with traditional unwrapping under Gaussian errors of (a) 3 mm, (b) 5 mm, and (c) 7 mm.

subsidence trough can be correctly restored, and the final standard deviation of the residual is 0.03 cm (0.077 rad).

C. Comparing the Advantages and Disadvantages of Different Models

The precision of the three models was compared. Fig. 3 shows that Mogi, PIM, and Okada models were able to recover the maximum subsidence information well with the 3-mm Gaussian error simulations. The performance of the three models is mostly consistent at different peak subsidence levels. The standard deviations of the final residuals were 0.03 cm (0.077 rad), 0.03 cm (0.075 rad), and 0.03 cm (0.074 rad) for the three deformation models, when dealing with the subsidence trough with 35-cm peak subsidence. These were significantly better than the results from the conventional unwrapping method (i.e., with SNAPHU alone). For the case of 5-mm Gaussian error simulations, Mogi, PIM, and Okada models were able to unwrap the subsidence trough precisely with peak subsidence up to 30 cm (67.9 rad),

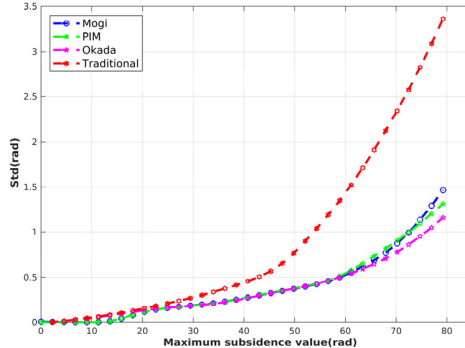


Fig. 4. Comparison of Mogi, PIM, and Okada models and conventional method with synthetic C-band interferogram generated from the L-band DInSAR results.

and the precision significantly degraded after that. For the case of 7-mm Gaussian error simulation, Mogi, PIM, and Okada models can only recover the 20-cm (45.3 rad) counterpart precisely, with much greater precision degrading rate. The standard deviations of the residuals were 0.07 cm (0.159 rad), 0.07 cm (0.152 rad), and 0.07 cm (0.151 rad) for the three deformation models, for recovering the subsidence trough with a peak subsidence of 20 cm.

Based on the above comparison, we find that the Okada model performs better at higher noise level [Fig. 3(c)]. Regardless of which model is used, the three models are able to solve the large gradient problem of the DInSAR results for mining area to some extent compared to the conventional method.

D. Experiment With the Synthetic C-Band Interferogram Generated From the L-Band DInSAR Results

Another simulation was conducted with the synthetic C-band interferogram. Instead of using mine subsidence trough obtained from Okada model inversion, an unwrapped L-band interferogram from real data was normalized directly. Two L-band ALOS (Advanced Land Observing Satellite) PALSAR (Phased Array type L-band SAR) images (frame: 649, path: 370), acquired on March 31, 2008, and May 16, 2008, covering the Metropolitan mine area on the east coast of Australia were used here.

The normalized data were multiplied by different coefficients (peak subsidence levels). The subsidence data with different subsidence levels were rewrapped into a C-band (5.55 cm) interferogram to simulate the C-band interferogram. Following the unwrapping strategy proposed in this letter, the results obtained by the inversion of the three models are compared with the results from the conventional unwrapping method. The simulation result is shown in Fig. 4. It can be seen that the precision of the conventional method is almost the same as that of the proposed strategy when the simulated peak subsidence data are less than 10 cm (22.6 rad). As the subsidence gradient increases, the degradation in precision increases faster than the proposed strategy. The Okada model appears to be more stable than the other two models with the peak subsidence of over 30 cm (67.9 rad).

IV. REAL InSAR DATA EXPERIMENT

The real data analysis was conducted with two C-band Sentinel-1 (track: 142) IW images, covering Huainan coalfield

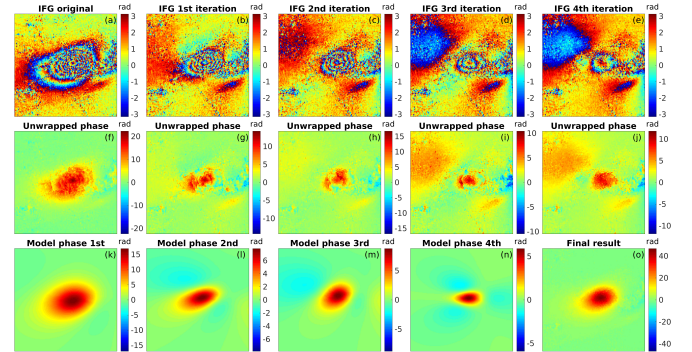


Fig. 5. Recovery of the subsidence trough in Kouzi Dong mine area by Okada model inversion. (a) Original interferogram. (b), (c), (d), and (e) Residual interferogram after the first, second, third, and fourth iterations, respectively. (f), (g), (h), (i), and (j) Unwrapped phase of (a), (b), (c), (d), and (e), respectively. (k), (l), (m), and (n) Modeled phase of (f), (g), (h), and (i), respectively. (o) Final result obtained using the proposed strategy.

of Anhui province, China. Fig. 5 shows the subsidence trough caused by underground coal mining at one of the workfaces in Kouzi Dong mine.

It can be seen in Fig. 5 that the unwrapped result from the first iteration (i.e., the conventional unwrapping approach) obviously underestimated subsidence. However, it can be seen that through the strategy proposed in this letter, after a number of iterations using the Okada model (i.e., four inversions), the center of the subsidence trough can be recovered. The peak subsidence observed from the approach with Okada model is 20.9 cm (47.2 rad), while the maximum recoverable subsidence at the subsidence center is only 9.9 cm (22.3 rad) with the conventional method. The Mogi and PIM counterparts are 46.84 and 46.83 rad, respectively. The inversion parameters for the Mogi, PIM, and Okada models are shown in Tables SI, SII, and SIII, respectively. The comparison of subsidence troughs derived from the three models with traditional phase unwrapping and the InSAR unwrapped phase from the proposed strategy is shown in Fig. S1.

V. DISCUSSION

Through the study of the simulated and real data, it is found that the proposed strategy can effectively address the phase saturation problem with all three models. The Okada model seems slightly more reliable for solving the large-scale subsidence in the mining area, followed by PIM model and Mogi model based on the results obtained. A reason could be that the Okada model is more complex and more adaptable. It needs to be noted that the Mogi model is relatively simple. Compared to the other two models, in the case when dealing with interferogram with large error, the Mogi model needs to go through more iterations to achieve better results. However, since the number of test cases used in this letter is limited, more test cases should be conducted for a more reliable assessment on the performance of the three models in the future.

In this letter, Okada, PIM, and Mogi are used to investigate the feasibility of the proposed strategy for mine subsidence mapping. However, other deformation models can also be used with the proposed strategy.

VI. CONCLUSION

The large subsidence gradient caused by underground mining has always been an important factor limiting the operational use of InSAR technology for mine subsidence mapping. This letter proposed an unwrapping strategy that can effectively address the phase saturation problem due to the excessive subsidence gradient. Compared with other studies, the proposed strategy of separating large gradient subsidence signals and small subsidence signals through multiple model inversion is an efficient solution especially when the accurate model parameters are not known. Both simulation and real data analyses have been conducted, suggesting that the proposed strategy is able to restore the phase at the subsidence center with better precision than the conventional method, which shows the significant advantage of the proposed strategy.

Subsequent research will further bring different models into the long-term sequence InSAR and analyze the dynamic mechanism of subsidence in the mining area and the performance of different models under long-term sequence conditions [34].

ACKNOWLEDGMENT

The authors thank the Earth Remote Sensing Data Analysis Center (ERSDAC) for providing the ALOS PALSAR data and European Space Agency for providing the Sentinel-1 data.

REFERENCES

- [1] H. A. Zebker and R. M. Goldstein, "Topographic mapping from interferometric synthetic aperture radar observations," *J. Geophys. Res.*, vol. 91, no. B5, p. 4993, 1986.
- [2] E. Rodriguez *et al.*, "An assessment of the SRTM topographic products," Jet Propuls. Lab., Pasadena, CA, USA, Tech. Rep. JPL D-31639, 2005.
- [3] D. Massonnet *et al.*, "The displacement field of the landers earthquake mapped by radar interferometry," *Nature*, vol. 364, no. 6433, pp. 138–142, Jul. 1993.
- [4] H. A. Zebker, P. A. Rosen, R. M. Goldstein, A. Gabriel, and C. L. Werner, "On the derivation of coseismic displacement fields using differential radar interferometry: The landers earthquake," *J. Geophys. Res., Solid Earth*, vol. 99, no. B10, pp. 19617–19634, Oct. 1994.
- [5] H. Wang *et al.*, "Sentinel-1 observations of the 2016 menyuan earthquake: A buried reverse event linked to the left-lateral haiyuan fault," *Int. J. Appl. Earth Observ. Geoinf.*, vol. 61, pp. 14–21, Sep. 2017.
- [6] S. V. Samsonov, P. J. Gonzalez, K. F. Tiampo, N. D. Apos, and Oreye, "Modeling of fast ground subsidence observed in southern Saskatchewan (Canada) during 2008–2011," *Natural Hazards Earth Syst. Sci.*, vol. 14, no. 2, pp. 247–257, Feb. 2013.
- [7] A. A. Malinowska, W. T. Witkowski, A. Guzy, and R. Hejmanowski, "Mapping ground movements caused by mining-induced earthquakes applying satellite radar interferometry," *Eng. Geol.*, vol. 246, pp. 402–411, Nov. 2018.
- [8] A. H.-M. Ng *et al.*, "Mapping accumulated mine subsidence using small stack of SAR differential interferograms in the southern coalfield of new south Wales, Australia," *Eng. Geol.*, vol. 115, nos. 1–2, pp. 1–15, Sep. 2010.
- [9] M. Ilieva *et al.*, "Mining deformation life cycle in the light of InSAR and deformation models," *Remote Sens.*, vol. 11, no. 7, p. 745, 2019.
- [10] L. Bateson, F. Cigna, D. Boon, and A. Sowter, "The application of the intermittent SBAS (ISBAS) InSAR method to the south Wales coalfield, UK," *Int. J. Appl. Earth Observ. Geoinf.*, vol. 34, pp. 249–257, Feb. 2015.
- [11] R. M. Goldstein, H. A. Zebker, and C. L. Werner, "Satellite radar interferometry: Two-dimensional phase unwrapping," *Radio Sci.*, vol. 23, no. 4, pp. 713–720, Jul. 1988.
- [12] H. Wu, H. Wang, X. Huang, C. Pagli, and Z. Yang, "Improving the coherence of interferograms of mining subsidence by oversampling," *J. Guangdong Univ. Technol.*, vol. 32, no. 3, pp. 123–126, Aug. 2015.
- [13] A. H.-M. Ng, L. Ge, Z. Du, S. Wang, and C. Ma, "Satellite radar interferometry for monitoring subsidence induced by longwall mining activity using radarsat-2, Sentinel-1 and ALOS-2 data," *Int. J. Appl. Earth Observ. Geoinf.*, vol. 61, pp. 92–103, Sep. 2017.
- [14] B. Q. Chen, K. Deng, and H. D. Fan, "Joint InSAR and three-dimensional laser scanning technology to monitor large gradient deformation in mining area," *Bull. Surv. Mapping*, vol. S1, pp. 88–94, Apr. 2014.
- [15] D. Ou, K. Tan, Q. Du, Y. Chen, and J. Ding, "Decision fusion of D-InSAR and pixel offset tracking for coal mining deformation monitoring," *Remote Sens.*, vol. 10, no. 7, p. 1055, 2018.
- [16] H.-D. Fan, W. Gu, Y. Qin, J.-Q. Xue, and B.-Q. Chen, "A model for extracting large deformation mining subsidence using D-InSAR technique and probability integral method," *Trans. Nonferrous Met. Soc. China*, vol. 24, no. 4, pp. 1242–1247, Apr. 2014.
- [17] Z. F. Yang, Z. W. Li, J. J. Zhu, J. Hu, Y. J. Wang, and G. L. Chen, "InSAR-based model parameter estimation of probability integral method and its application for predicting mining-induced horizontal and vertical displacements," *IEEE Trans. Geosci. Remote Sens.*, vol. 54, no. 8, pp. 4818–4832, Aug. 2016.
- [18] Z. Yang, Z. Li, J. Zhu, H. Yi, J. Hu, and G. Feng, "Deriving dynamic subsidence of coal mining areas using InSAR and logistic model," *Remote Sens.*, vol. 9, no. 2, p. 125, 2017.
- [19] X. Diao, K. Wu, Y. Xu, D. Zhou, and R. Chen, "Prediction-based phase unwrapping for differential interferograms of coal mining areas using a stochastic medium model," *Remote Sens. Lett.*, vol. 9, no. 5, pp. 477–486, May 2018.
- [20] H. Fan, L. Lu, and Y. Yao, "Method combining probability integration model and a small baseline subset for time series monitoring of mining subsidence," *Remote Sens.*, vol. 10, no. 9, p. 1444, 2018.
- [21] J. Blachowski, W. Milczarek, and P. Stefanik, "Deformation information system for facilitating studies of mining-ground deformations, development, and applications," *Natural Hazards Earth Syst. Sci.*, vol. 14, no. 7, pp. 1677–1689, 2014.
- [22] K. Mogi, "Relations between the eruptions of various volcanoes and the deformations of the ground surfaces around them," *Bull. Earthq. Res. Inst.*, vol. 36, pp. 99–134, Jan. 1958.
- [23] Y. Okada, "Surface deformation due to shear and tensile faults in a half-space," *Bull. Seismol. Soc. Amer.*, vol. 75, no. 4, pp. 1135–1154, Aug. 1985.
- [24] J. Litwiniszyn, "Application of the equation of stochastic processes to mechanics of loose bodies," *Arch. Mech. Stos.*, vol. 8, no. 4, pp. 393–411, 1956.
- [25] A. H.-M. Ng, H.-C. Chang, L. Ge, C. Rizos, and M. Omura, "Assessment of radar interferometry performance for ground subsidence monitoring due to underground mining," *Earth, Planets Space*, vol. 61, no. 6, pp. 733–745, Jun. 2009.
- [26] R. M. Goldstein and C. L. Werner, "Radar interferogram filtering for geophysical applications," *Geophys. Res. Lett.*, vol. 25, no. 21, pp. 4035–4038, Nov. 1998.
- [27] Y. Fialko, M. Simons, and D. Agnew, "The complete (3-D) surface displacement field in the epicentral area of the 1999 $M_w 7.1$ Hector Mine Earthquake, California, from space geodetic observations," *Geophys. Res. Lett.*, vol. 28, no. 16, pp. 3063–3066, Aug. 2001.
- [28] H. Wang, L. Ge, C. Xu, and Z. Du, "3-D coseismic displacement field of the 2005 kashmir earthquake inferred from satellite radar imagery," *Earth, Planets Space*, vol. 59, no. 5, pp. 343–349, May 2007.
- [29] A. H.-M. Ng, L. Ge, K. Zhang, and X. Li, "Estimating horizontal and vertical movements due to underground mining using ALOS PALSAR," *Eng. Geol.*, vols. 143–144, pp. 18–27, Aug. 2012.
- [30] D. L. Carroll, "Genetic algorithms and optimizing chemical oxygen-iodine lasers," *Develop. Theor. Appl. Mech.*, vol. 18, no. 3, pp. 411–424, 1996.
- [31] S. Peng, *Coal Mine Ground Control*, 2nd ed. ed. New York, NY, USA: Wiley, 1986.
- [32] C. W. Chen and H. A. Zebker, "Phase unwrapping for large SAR interferograms: Statistical segmentation and generalized network models," *IEEE Trans. Geosci. Remote Sens.*, vol. 40, no. 8, pp. 1709–1719, Aug. 2002.
- [33] S. Jónsson, H. Zebker, P. Segall, and F. Amelung, "Fault slip distribution of the 1999 $M_{w} 7.1$ hector mine, California, Earthquake, estimated from Satellite radar and GPS measurements," *Bull. Seismol. Soc. Amer.*, vol. 92, no. 4, pp. 1377–1389, May 2002.
- [34] P. Li, D. Peng, Z. Tan, and K. Deng, "Study of probability integration method parameter inversion by the genetic algorithm," *Int. J. Mining Sci. Technol.*, vol. 27, no. 6, pp. 1073–1079, Nov. 2017.